HHS Public Access

Author manuscript

Ann Nucl Med. Author manuscript; available in PMC 2022 April 25.

Published in final edited form as:

Ann Nucl Med. 2017 December ; 31(10): 736–743. doi:10.1007/s12149-017-1205-0.

Uptake of AV-1451 in meningiomas

Tyler J. Bruinsma[1], **Derek R. Johnson**[1,2], **Ping Fang**[1], **Matthew Senjem**[1,3], **Keith A. Josephs**[2], **Jennifer L. Whitwell**[1], **Bradley F. Boeve**[2], **Mukesh K. Pandey**[1], **Kejal Kantarci**[1], **David T. Jones**[1,2], **Prashanthi Vemuri**[1], **Melissa Murray**[4], **Jonathan Graff-Radford**[2], **Christopher G. Schwarz**[1], **David S. Knopman**[2], **Ronald C. Petersen**[2], **Clifford R. Jack Jr.**[1], **Val J. Lowe**[1]

[1]Department of Radiology, Mayo Clinic, 200 First Street SW, Rochester, MN 55905, USA

[2]Department of Neurology, Mayo Clinic, Rochester, MN, USA

[3]Department of Information Technology, Mayo Clinic, Rochester, MN, USA

[4]Department of Neurology, Mayo Clinic, Jacksonville, FL, USA

Abstract

Aim—AV-1451 is an imaging agent labeled with the positron-emitting radiolabel Fluorine-18. 18F-AV-1451 binds paired helical filament tau (PHF-tau), a pathology related to Alzheimer's disease. In our study of AV-1451 uptake in the brains of cognitively normal subjects, we noted a case of a meningioma with visually significant uptake of AV-1451.

Objective—We initiated the present retrospective study to further examine cases of meningioma that underwent AV-1451 imaging.

Methods—We searched the patient records of 650 patients who had undergone AV-1451 at our institution for the keyword "meningioma" to identify potential cases. PET/CT and MRI results were visually reviewed and semi-quantitative analysis of PET was performed. A paired student's *t* test was run between background and tumor standard uptake values. Fisher's exact test was used to examine the association between AV-1451 uptake and presence of calcifications on CT.

Results—We identified 12 cases of meningioma, 58% (7/12) of which demonstrated uptake greater than background using both visual analysis and tumor-to-normal cortex ratios (T/N + 1.90 ± 0.83). The paired student's *t* test revealed no statistically significant difference between background and tumor standard uptake values ($p = 0.09$); however, cases with a T/N ratio greater than one showed statistically higher uptake in tumor tissue ($p = 0.01$). A significant association was noted between AV-1451 uptake and presence of calcifications ($p = 0.01$).

Conclusion—AV-1451 PET imaging should be reviewed concurrently with anatomic imaging to prevent misleading interpretations of PHF-tau distribution due to meningiomas.

Keywords

Meningioma; AV-1451; Imaging

Introduction

The imaging agent ^{18}F AV-1451 (T807) binds paired helical filament tau (PHF-tau), a protein associated with Alzheimer's disease (AD) for visualization in PET imaging [1–4]. The development of AV-1451 comes in response to developments in AD research that implicate tau accumulation as an important progressive pathology of the disease [1, 5–7]. Autoradiography of human brain samples indicates significant co-localization of AV-1451 and PHF-tau immunohistochemistry in adjacent sections and high selectivity for PHF-tau over amyloid-β plaques which show similar pathology [1, 8, 9]. Tau accumulation as indicated by AV-1451 is associated with cognitive deficits attributed to specific regions of the brain [5]. Off-target binding of AV-1451 in-vitro is negligible as assessed with a panel of 72 common CNS targets [1], but is more predominate in ex-vivo autoradiography samples [8, 9]. Non-target binding in-vivo is increasingly reported and constitutes a vital area of research as AV-1451 imaging progresses to clinical use.

Meningiomas are the most commonly reported primary brain tumor in the United States [10]. Roughly 90% of meningiomas are benign, implicating resection only in situations, where clinical symptoms are significant [11–13]. The remaining 10% of meningiomas are more aggressive, or in rare cases, malignant [12–14]. Meningiomas are commonly diagnosed through contrast-enhanced or unenhanced CT imaging and MR imaging, often as incidental findings [11]. On CT, meningiomas typically appear hyperdense or isodense to surrounding cortical tissue [15]. On MRI, meningiomas are isointense or mildly hypointense, but typically enhance with gadolinium [15]. Some meningiomas demonstrate visual calcification on imaging, improving visualization [16]. Positron-emission tomography (PET) of meningiomas is less common; however, [^{18}F] Fludeoxyglucose (FDG) imaging provides an option for determining the aggressiveness of malignant tumors [11, 17, 18]. [^{68}Ga] DOTATOC imaging provides superior contrast of tumor margins for pre-operative planning of resection, but is not specific to meningiomas [19, 20]. [^{11}C] methionine (MET) is equally non-specific to meningioma, but provides superior identification of primary brain tumors and recurrence of tumors as compared to FDG [20–23]. Dynamic acquisition and analysis of MET uptake increase the differential diagnosis capabilities of the tracer as dynamic decreases of the maximum T/N ratio are noted in meningiomas but not glioblastomas or lymphomas [24]. Additional experimental PET tracers are generally non-specific to meningiomas and presently do not increase diagnostic confidence [19, 20, 23, 25–36].

In the process of reviewing AV-1451 scans from ongoing research studies, we incidentally identified significant uptake of AV-1451 in a meningioma. We hypothesize that additional cases of meningioma will show similar uptake. The present study was initiated to retrospectively examine AV-1451 uptake in meningiomas to determine the characteristics of the tracer in meningiomas of various sizes and types.

Methods

Case selection

Cases were selected from a cohort of 650 patients who had volunteered for a research imaging study with the radiotracer AV-1451. All patients signed proper informed consent for research imaging and the research trial was approved by the Institutional Review Board of the institution. The medical records of the 650 patients were searched for the keyword “meningioma”. Patients were included in the present study if they were found to have a meningioma on anatomic imaging.

Imaging protocols

The day prior to the imaging study, water consumption was encouraged to induce more rapid clearance of the radioisotope. Subjects were injected with 370 ± 37 MBq of ^{18}F-AV-1451 intravenously. Imaging was delayed for 80–100 min following injection to allow for uptake of the radiotracer. PET/CT scans were then acquired on the GE Discovery RX or Discovery 690XT (General Electric Healthcare; Waukesha, WI, USA) cameras. CT images were reconstructed in a transaxial slice orientation with a slice thickness of 3.75 and interval of 3.27 or 1.96 mm depending on the scanner. Forty-seven or seventy-nine slices were obtained again dependent on the scanner and interval used. For CT imaging, kVp was 120 and mA was 35–40. On PET, four frames of 5 min each were obtained to correct for patient motion and were summed. A 3D OSEM iterative algorithm was used for reconstruction and a 5.0 mm post-filter was applied. Attenuation correction was measured using the CT obtained prior to PET. MRIs were performed at 3 T using an eight-channel phased array coil on all participants. MRI methods have been previously described [37].

Radiosynthesis of AV-1451

^{18}F-AV-1451 was produced by the radiopharmacy at Mayo Clinic in Rochester, MN following the protocols previously described [8].

Image analysis

Non-contrast MR images obtained for study purposes were interpreted by a CAQ-certified neuroradiologist prior to the initiation of the retrospective review. Additional diagnostic MRI examinations with intravenous contrast were reviewed when available. Probable meningiomas were confirmed by consensus. Tumor measurements were made with the OsiriX Open-Source PACS Workstation, 64-bit version 7.5 (Pixmeo; Geneva, Switzerland). MR scans were compared along-side PET/CT in cases, where meningiomas were difficult to identify on CT.

PET/CT scans were reviewed visually for uptake greater than background and quantified with the AW VolumeShare 2 software (General Electric Healthcare; Waukesha, WI, USA). Calcification was visually assessed using CT. Existence of meningioma was informed, but the presence of calcification on CT was blinded. The maximum standard uptake value (SUV_{max}) was determined in the meningioma and a randomly selected region of interest (ROI) in normal brain tissue in the occipital region of the same slice as the meningioma ROI. A circular ROI was drawn to encompass the entirety of the meningioma to assess

tumor SUV_{max}. The ROI was then translated to normal cortical tissue in the same slice for assessment of the normal SUV_{max}. Axial slices were visually selected based on the greatest uptake with multiple slices sampled to quantitatively confirm the maximum uptake. ROIs were set by one individual (TJB) under the guidance of an experienced nuclear medicine physician (VJL). Tumor-to-normal tissue ratios (*T*/*N*) were also calculated for standardized comparison. A *T*/*N* ratio greater than one was considered positive for AV-1451 uptake. SUV_{max} was calculated by the AW VolumeShare 2 software using the following method: SUVmax = [Max ROI activity (MBq/g)]/[Injected dose (MBq)/body weight in grams].

Autoradiography and immunohistochemistry

Post-mortem samples of meningiomas were selected from the Mayo Clinic Brain Bank. Samples obtained were from patients who were not scanned in the PET/CT trial, no such samples were available. AV-1451 autoradiography and PHF-tau immunohistochemistry (IHC) were performed as previously described on six samples of meningioma [8]. A standard hematoxylin and eosin (H&E) stain was also evaluated for calcified areas of interest.

Statistical analysis

A one-tailed, paired student's *T* test was performed to assess variance between tumor and background SUV maximums. Fisher's exact test was performed to examine the association between AV-1451 uptake and the presence of calcification.

Results

Twelve cases of meningioma were selected following the medical record search. Subjects were on average 75 years at the time of AV-1451 scanning (range 54–83). Five were male and seven were female. One subject (case 11) was diagnosed with amnestic mild cognitive impairment, while all others were cognitively normal. Biopsy diagnosis was not performed on any of the meningiomas. Detailed subject information is noted in Table 1.

All cases were hypointense or isointense on non-contrast T1-weighted MR imaging. The vast majority of tumors were isointense or hypointense on T2-weighted images, with the exception of a single tumor (Case 6) which was mildly T2 hyperintense. No hyper-intensity or edema in surrounding brain tissue was noted in any cases.

Seven cases demonstrated visual evidence of AV-1451 uptake by the meningioma and observably greater SUV maximum values (58%) (Fig. 1). Five cases showed no uptake in the meningioma with SUV maximums lower than background (Fig. 2). All cases of positive visual uptake also noted calcifications on CT imaging, while only one case negative for visual uptake noted calcifications. Upon statistical analysis using Fisher's exact test, a significant association between AV-1451 visual uptake and calcification was noted ($p = 0.01$). Table 1 includes all SUV_{max} data and visual assessment results. A paired student's *t* test revealed no significant differences in SUV maximum as compared to background ROIs ($p = 0.09$); however, for the seven tumors with *T*/*N* ratios greater than one, the paired *t* test results were significant ($p = 0.01$) indicating significantly greater uptake in tumor as

compared to background. The average *T*/*N* ratio for all cases was 1.43. In the group of meningiomas that visually demonstrate stronger binding, the average T/N ratio was 1.9.

Tissue samples from six post-mortem cases were examined; three were highly calcified and three showed minimal calcification. No cases entirely devoid of psammoma bodies (indicative of calcification) were available. Calcifications observed on H&E were co-localized with stronger binding in autoradiography images by visual comparison. PHF-Tau staining revealed negligible binding in all samples. Figures 3, 4, 5 depict three representative cases for a correlative comparison.

Discussion

Visually observable uptake of AV-1451 was seen in over half of meningiomas. This finding is essential to consider when performing quantitative analysis of AV-1451 images in brain regions, where meningiomas are present. When performing regional AV-1451 analysis, especially when using MRI templates or other non-individual ROI segmentation methods, uptake of AV-1451 in meningiomas within a region may lead to improper characterization of AV-1451 uptake as spuriously representing pathologic PHF-tau in the brain region. Group uptake in meningiomas by SUV analysis was not significantly higher than normal background uptake; however, the sub-group demonstrating visual hyper-intensity did show significantly higher uptake. This is of particular interest as quantitative analysis of AV-1451 imaging develops.

Meningiomas are effectively diagnosed through CT and MR imaging particularly when calcification is present. Given the strong correlation between AV-1451 uptake and calcified meningiomas in the present study, the potential for AV-1451 to improve meningioma diagnosis is limited. In addition, MET and DOTATOC imaging provides superior visualization of tumor margins with dynamic MET imaging also providing some differential diagnostic capabilities; limiting any added benefit from AV-1451 imaging of meningioma. While AV-1451 is not effective for the characterization of meningiomas, it is an interesting source of off-target binding. The mechanism of AV-1451 uptake by meningiomas is not easily elucidated. Meningiomas are not known to accumulate tau protein, particularly that of AD origin [38]. Post-mortem immunostaining of 15 cases of meningioma for tau revealed no immunoreactivity within tumor margins which is consistent with our findings in six cases of meningioma [38]. One case of positive staining was previously recorded with the cerebral tissue surrounding and compressed by the meningioma staining darkly for tau but still lacked tau infiltration into the meningioma [38]. The presence of PHF-tau within meningiomas does not appear to be a viable explanation of the off-target binding that we have noted.

It is possible that meningiomas present with paired helical filaments of other proteins or other crystalline structures similar to those noted in AD that may serve as surrogates for AV-1451 binding. All seven cases positive for AV-1451 uptake demonstrated calcification on CT image analysis, suggesting that calcifications may provide the crystalline structure necessary for AV-1451 binding. Autoradiographic and H&E analysis of meningioma slices supports this hypothesis as calcifications were co-localized with elevated AV-1451 binding

but not with PHF-tau IHC reactivity. Previously reported post-mortem autoradiographic evaluation of AV-1451 in brain samples from Alzheimer's disease cases indicated off-target binding in calcifications located in the choroid plexsus further supporting this conjecture [8]. One case that was negative for AV-1451 uptake did express distinct calcification on CT indicating the potential for a more complicated binding mechanism potentially related to previously defined off-target binding such as neuromelanin or hemorrhagic lesions [9]. Similar uptake of the amyloid PET radiotracer, Pittsburgh compound B (PiB) in meningiomas is noted in our practice (unpublished) and in previously published works [39, 40]. Understanding PiB binding better could shed light on similar off-target mechanisms of AV-1451 accumulation in meningiomas.

Case 8 (Fig. 1) depicts a meningioma in which the uptake of AV-1451 did not encompass the entire tumor area. Given the premise that AV-1451 binds calcifications, we hypothesize that the core of the tumor was more densely calcified than the periphery leading to the observed pattern of uptake. Case 8 did not require surgical excision, so no tumor slices are available for ex-vivo assessment with H&E staining. CT imaging indicates variable calcification throughout the meningioma, but without ex-vivo analysis, density of psammoma bodies is difficult to assess.

Further pathological studies of meningiomas are necessary to determine the exact mechanism that causes significant AV-1451 uptake in some meningiomas. The selective nature of this uptake in 58% (7/12) of our reported cases provides evidence that meningiomas need to be considered as possible causes of false positive uptake on AV-1451 scans. With a greater understanding of the unique pathology of differing meningiomas, AV-1451 imaging and off-target binding may be better understood.

Conclusion

Our study demonstrated visual uptake of AV-1451 in 58% (7/12) of meningiomas. Analysis of AV-1451 PET images should include review of regions that include meningiomas to avoid misleading interpretations about the presence of PHF-tau in the brain. To this end, review of individual anatomic imaging should accompany AV-1451 PET imaging.

Financial support

This research was supported by NIH Grants, P50 AG016574, R01 NS89757, R01 NS089544, R01 DC10367, U01 AG006786, R21 NS094489, by the Robert Wood Johnson Foundation, The Elsie and Marvin Dekelboum Family Foundation, The Liston Family Foundation and by the Robert H. and Clarice Smith and Abigail van Buren Alzheimer's Disease Research Program, The GHR Foundation, Foundation Dr. Corinne Schuler and the Mayo Foundation.

References

1. Xia CF, Arteaga J, Chen G, Gangadharmath U, Gomez LF, Kasi D, et al. [(18)F]T807, a novel tau positron emission tomography imaging agent for Alzheimer's disease. Alzheimers Dement. 2013;9(6):666–76. [PubMed: 23411393]
2. Chien DT, Bahri S, Szardenings AK, Walsh JC, Mu F, Su MY, et al. Early clinical PET imaging results with the novel PHF-tau radioligand [F-18]-T807. J Alzheimers Dis. 2013;34(2):457–68. [PubMed: 23234879]

3. Villemagne VL, Okamura N. Tau imaging in the study of ageing, Alzheimer's disease, and other neurodegenerative conditions. Curr Opin Neurobiol. 2016;36:43–51. [PubMed: 26397020]
4. Scholl M, Lockhart SN, Schonhaut DR, O'Neil JP, Janabi M, Ossenkoppele R, et al. PET imaging of tau deposition in the aging human brain. Neuron. 2016;89(5):971–82. [PubMed: 26938442]
5. Ossenkoppele R, Schonhaut DR, Scholl M, Lockhart SN, Ayakta N, Baker SL, et al. Tau PET patterns mirror clinical and neuroanatomical variability in Alzheimer's disease. Brain. 2016;139(Pt 5):1551–67. [PubMed: 26962052]
6. Villemagne VL, Fodero-Tavoletti MT, Masters CL, Rowe CC. Tau imaging: early progress and future directions. Lancet Neurol. 2015;14(1):114–24. [PubMed: 25496902]
7. Dani M, Brooks DJ, Edison P. Tau imaging in neurodegenerative diseases. Eur J Nucl Med Mol Imaging. 2016;43(6):1139–50. [PubMed: 26572762]
8. Lowe VJ, Curran G, Fang P, Liesinger AM, Josephs KA, Parisi JE, et al. An autoradiographic evaluation of AV-1451 Tau PET in dementia. Acta Neuropathol Commun. 2016;4(1):58. [PubMed: 27296779]
9. Marquie M, Normandin MD, Vanderburg CR, Costantino IM, Bien EA, Rycyna LG, et al. Validating novel tau positron emission tomography tracer [F-18]-AV-1451 (T807) on postmortem brain tissue. Ann Neurol. 2015;78(5):787–800. [PubMed: 26344059]
10. Wiemels J, Wrensch M, Claus EB. Epidemiology and etiology of meningioma. J Neurooncol. 2010;99(3):307–14. [PubMed: 20821343]
11. Pamir MN, Black PM, Fahlbusch R. Meningiomas: a comprehensive text, vol xxiii. Philadelphia: Saunders/Elsevier; 2010. p. 773.
12. Black PM. Meningiomas. Neurosurgery. 1993;32(4):643–57. [PubMed: 8474655]
13. Kleihues P, Louis DN, Scheithauer BW, Rorke LB, Reifenberger G, Burger PC, et al. The WHO classification of tumors of the nervous system. J Neuropathol Exp Neurol. 2002;61(3):215–25 (discussion 26–29). [PubMed: 11895036]
14. Bondy M, Ligon BL. Epidemiology and etiology of intracranial meningiomas: a review. J Neurooncol. 1996;29(3):197–205. [PubMed: 8858525]
15. Fogh SE, Johnson DR, Barker FG, Brastianos PK, Clarke JL, Kaufmann TJ, et al. Case-based review: meningioma. Neuro Oncol Pract. 2016;3(2):120–34.
16. Sheporaitis LA, Osborn AG, Smirniotopoulos JG, Clunie DA, Howieson J, D'Agostino AN. Intracranial meningioma. AJNR Am J Neuroradiol. 1992;13(1):29–37. [PubMed: 1595462]
17. Di Chiro G, Hatazawa J, Katz DA, Rizzoli HV, De Michele DJ. Glucose utilization by intracranial meningiomas as an index of tumor aggressivity and probability of recurrence: a PET study. Radiology. 1987;164(2):521–6. [PubMed: 3496626]
18. Lee JW, Kang KW, Park SH, Lee SM, Paeng JC, Chung JK, et al. 18F-FDG PET in the assessment of tumor grade and prediction of tumor recurrence in intracranial meningioma. Eur J Nucl Med Mol Imaging. 2009;36(10):1574–82. [PubMed: 19377904]
19. Rachinger W, Stoecklein VM, Terpolilli NA, Haug AR, Ertl L, Poschl J, et al. Increased 68 Ga-DOTATATE uptake in PET imaging discriminates meningioma and tumor-free tissue. J Nucl Med. 2015;56(3):347–53. [PubMed: 25635133]
20. Chung JK, Kim YK, Kim SK, Lee YJ, Paek S, Yeo JS, et al. Usefulness of 11C-methionine PET in the evaluation of brain lesions that are hypo- or isometabolic on 18F-FDG PET. Eur J Nucl Med Mol Imaging. 2002;29(2):176–82. [PubMed: 11926379]
21. Tripathi M, Sharma R, Varshney R, Jaimini A, Jain J, Souza MM, et al. Comparison of F-18 FDG and C-11 methionine PET/CT for the evaluation of recurrent primary brain tumors. Clin Nucl Med. 2012;37(2):158–63. [PubMed: 22228339]
22. Grosu AL, Weber WA, Astner ST, Adam M, Krause BJ, Schwaiger M, et al. 11C-methionine PET improves the target volume delineation of meningiomas treated with stereotactic fractionated radiotherapy. Int J Radiat Oncol Biol Phys. 2006;66(2):339–44. [PubMed: 16765533]
23. Nyberg G, Bergstrom M, Enblad P, Lilja A, Muhr C, Langstrom B. PET-methionine of skull base neuromas and meningiomas. Acta Otolaryngol. 1997;117(4):482–9. [PubMed: 9288200]
24. Aki T, Nakayama N, Yonezawa S, Takenaka S, Miwa K, Asano Y, et al. Evaluation of brain tumors using dynamic 11C-methionine-PET. J Neurooncol. 2012;109(1):115–22. [PubMed: 22528799]

25. Lau EW, Drummond KJ, Ware RE, Drummond E, Hogg A, Ryan G, et al. Comparative PET study using F-18 FET and F-18 FDG for the evaluation of patients with suspected brain tumour. J Clin Neurosci. 2010;17(1):43–9. [PubMed: 20004582]
26. Pruim J, Willemsen AT, Molenaar WM, van Waarde A, Paans AM, Heesters MA, et al. Brain tumors: L-[1-C-11]tyrosine PET for visualization and quantification of protein synthesis rate. Radiology. 1995;197(1):221–6. [PubMed: 7568827]
27. Rutten I, Cabay JE, Withofs N, Lemaire C, Aerts J, Baart V, et al. PET/CT of skull base meningiomas using 2–18F-fluoro-L-tyrosine: initial report. J Nucl Med. 2007;48(5):720–5. [PubMed: 17475959]
28. Moresco RM, Scheithauer BW, Lucignani G, Lombardi D, Rocca A, Losa M, et al. Oestrogen receptors in meningiomas: a correlative PET and immunohistochemical study. Nucl Med Commun. 1997;18(7):606–15. [PubMed: 9342097]
29. Fujimoto M, Yoshino E, Hirakawa K, Fujimoto J, Tamaya T. Estrogen receptors in brain tumors. Clin Neuropharmacol. 1984;7(4):357–62. [PubMed: 6509447]
30. Nathoo F, Dean CB. A mixed mover-stayer model for spatiotemporal two-state processes. Biometrics. 2007;63(3):881–91. [PubMed: 17825018]
31. Meewes C, Bohuslavizki KH, Krisch B, Held-Feindt J, Henze E, Clausen M. Molecular biologic and scintigraphic analyses of somatostatin receptor-negative meningiomas. J Nucl Med. 2001;42(9):1338–45. [PubMed: 11535722]
32. Henze M, Dimitrakopoulou-Strauss A, Milker-Zabel S, Schuhmacher J, Strauss LG, Doll J, et al. Characterization of 68 Ga-DOTA-D-Phe1-Tyr3-octreotide kinetics in patients with meningiomas. J Nucl Med. 2005;46(5):763–9. [PubMed: 15872348]
33. Gehler B, Paulsen F, Oksuz MO, Hauser TK, Eschmann SM, Bares R, et al. [68Ga]-DOTATOC-PET/CT for meningioma IMRT treatment planning. Radiat Oncol. 2009;4:56. [PubMed: 19922642]
34. Pettinato C, Sarnelli A, Di Donna M, Civollani S, Nanni C, Montini G, et al. 68 Ga-DOTANOC: biodistribution and dosimetry in patients affected by neuroendocrine tumors. Eur J Nucl Med Mol Imaging. 2008;35(1):72–9. [PubMed: 17874094]
35. Nathoo N, Ugokwe K, Chang AS, Li L, Ross J, Suh JH, et al. The role of 111indium-octreotide brain scintigraphy in the diagnosis of cranial, dural-based meningiomas. J Neurooncol. 2007;81(2):167–74. [PubMed: 16850106]
36. Henze M, Schuhmacher J, Hipp P, Kowalski J, Becker DW, Doll J, et al. PET imaging of somatostatin receptors using [68GA] DOTA-D-Phe1-Tyr3-octreotide: first results in patients with meningiomas. J Nucl Med. 2001;42(7):1053–6. [PubMed: 11438627]
37. Lowe VJ, Kemp BJ, Jack CR Jr, Senjem M, Weigand S, Shiung M, et al. Comparison of 18F-FDG and PiB PET in cognitive impairment. J Nucl Med. 2009;50(6):878–86. [PubMed: 19443597]
38. Miyazono M, Iwaki T, Kitamoto T, Shin RW, Fukui M, Tateishi J. Widespread distribution of tau in the astrocytic elements of glial tumors. Acta Neuropathol. 1993;86(3):236–41. [PubMed: 8213081]
39. Yamamoto Y, Maeda Y, Kawai N, Kudomi N, Nishiyama Y. Unexpected finding of cerebral meningioma on (11)C-PiB PET. Clin Nucl Med. 2013;38(4):292–3. [PubMed: 23429388]
40. Kim HY, Kim J, Lee JH. Incidental finding of meningioma on C11-PIB PET. Clin Nucl Med. 2012;37(2):e36–7. [PubMed: 22228363]

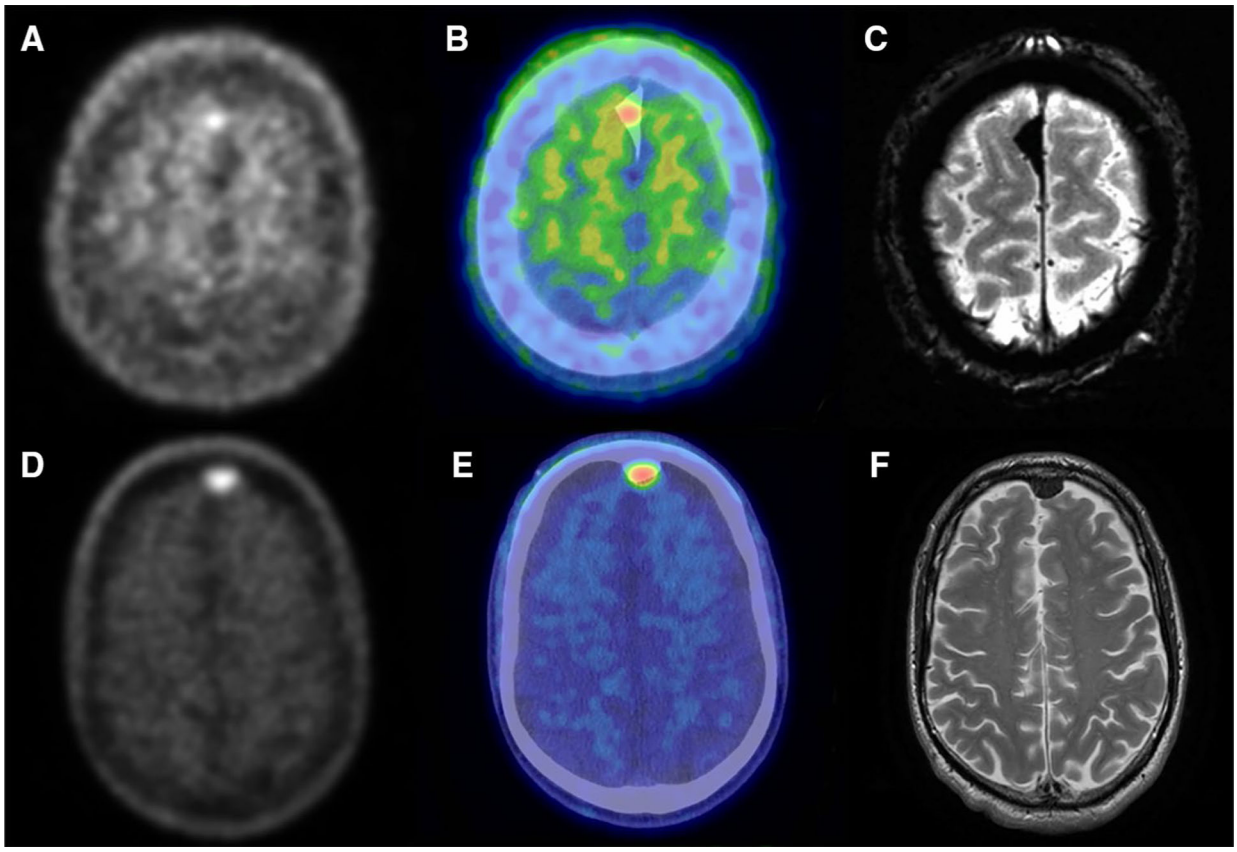

Fig. 1.

Two representative cases, patient 8 (*top*) and patient 12 (*bottom*), of meningioma with visible uptake of AV-1451. Axial slices of PET (**a, d**) and PET/CT fusion (**b, e**) show uptake that is co-localized with meningioma on MR (**c, f**). MR images are Axial Gradient Echo (**c**) and T2 weighted (**f**)

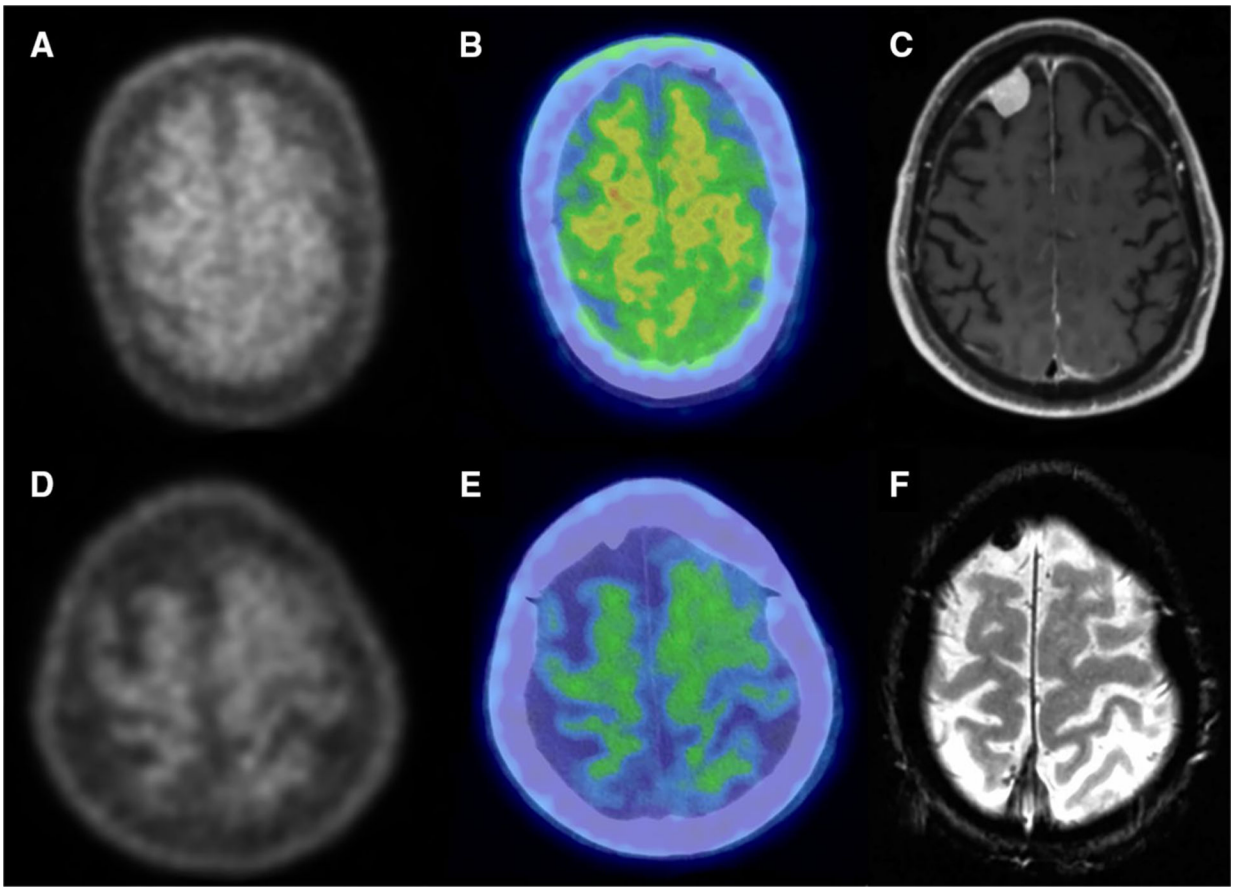

Fig. 2.

Two representative cases, patients 5 (*top*) and 6 (*bottom*), of meningioma lacking uptake of AV-1451. Axial slices of PET (**a, d**) and PET/CT fusion (**b, e**) show uptake at or below normal uptake in regions identified as meningioma by MR (**c, f**). MR images are axial T1-weighted post-gadolinium (**c**) and axial gradient echo (**f**)

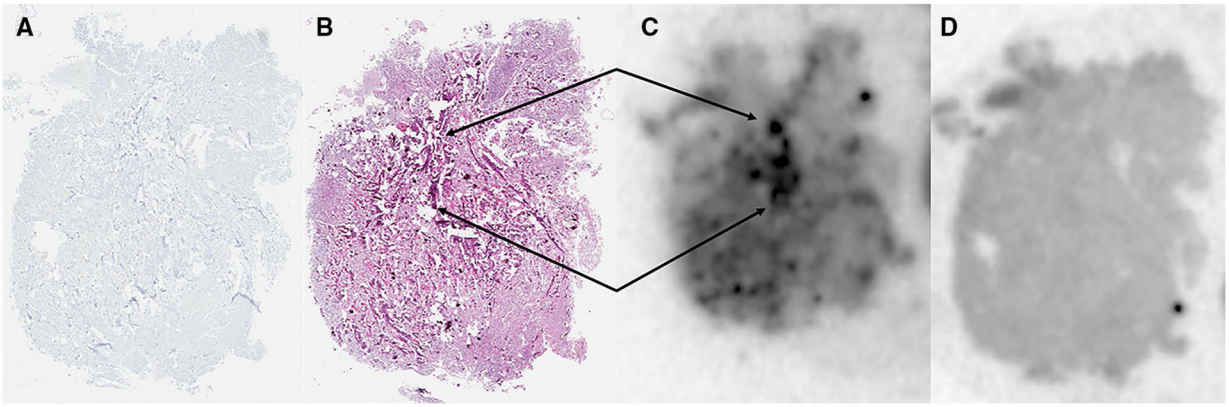

Fig. 3.

Correlative PHF-Tau IHC (**a**), H&E staining (**b**), and AV-1451 autoradiography without (**c**) and with blocking (**d**) of a meningioma positive for calcifications. *Arrows* indicate highly calcified areas co-localized on autoradiography and H&E staining

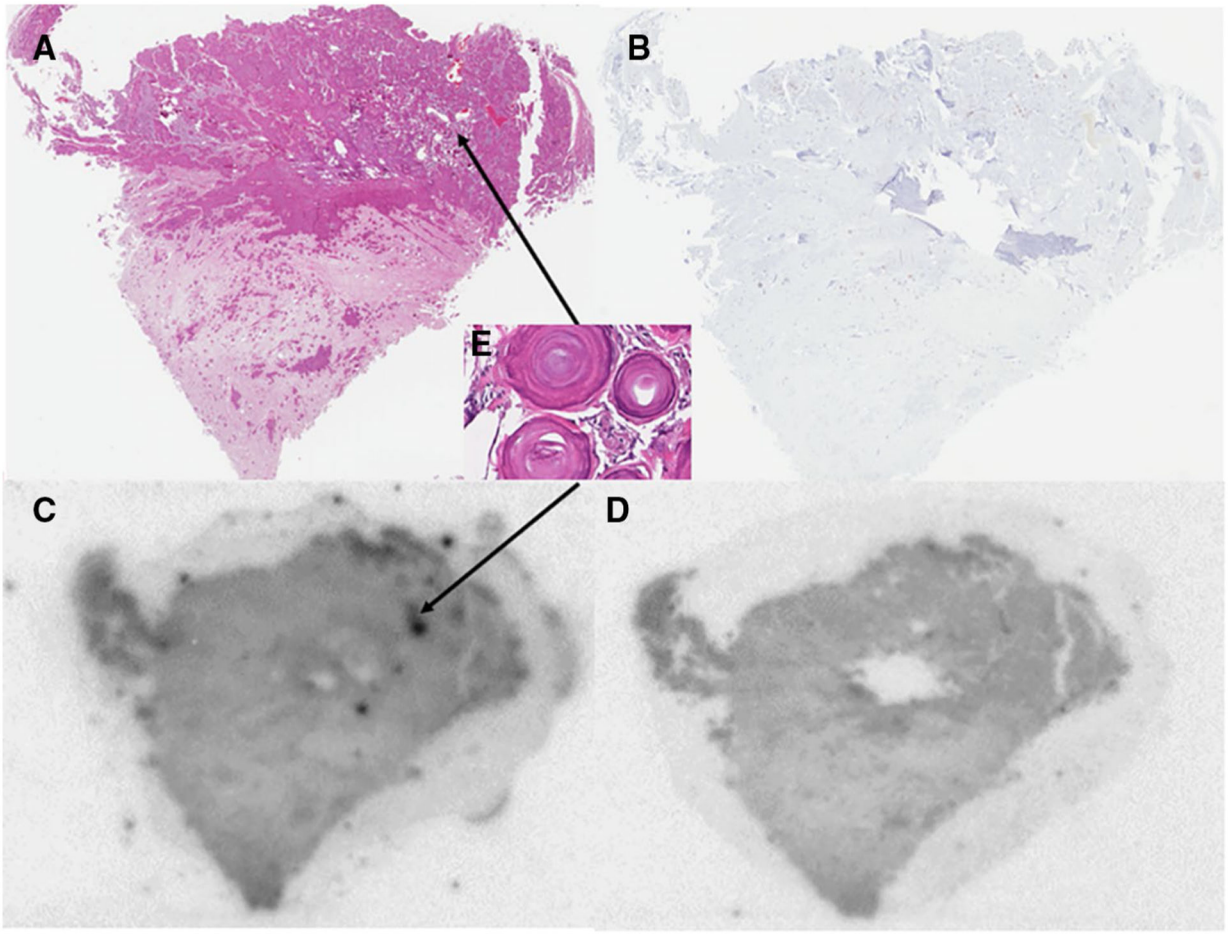

Fig. 4.

Correlative H&E staining (**a**), PHF-Tau IHC (**b**), and AV-1451 autoradiography without (**c**) and with blocking (**d**) of a meningioma positive for calcifications. *Inset* **e** depicts zoomed-in analysis of psammoma body calcifications that correlate with increased AV-1451 signal seen on autoradiography

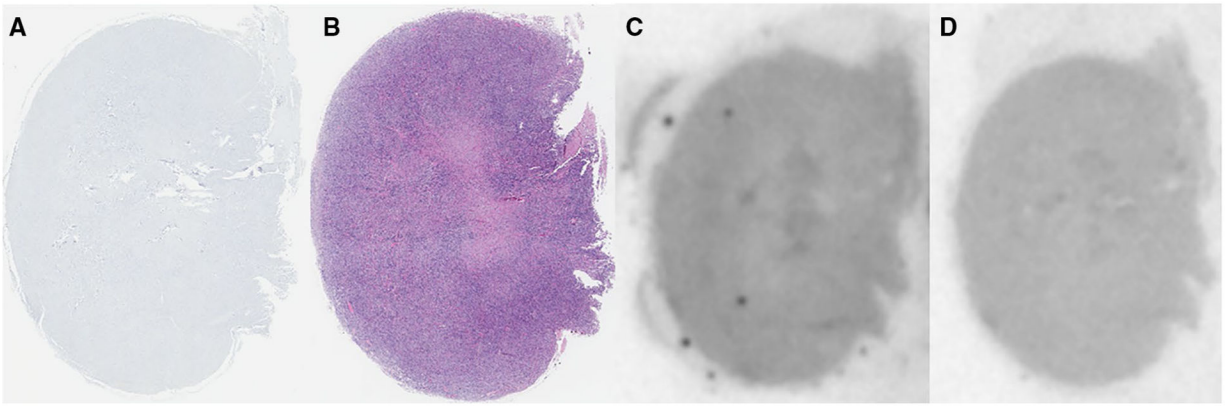

Fig. 5.

Correlative PHF-Tau IHC (**a**), H&E staining (**b**), and AV-1451 autoradiography without (**c**) and with blocking (**d**) of a meningioma negative for calcifications

Table 1

Patient and meningioma characteristics and semi-quantitative PET results

Pt.	Age	Sex	Visual assessment of AV-1451 PET	Tumor SUV	BKGD SUV	T/N	Size from MRI (cm)	Calcification present
1	81	F	−	1.1	1.3	0.85	1.1 × 1.0 × 1.1	−
2	81	F	+	2	1.3	1.54	1.9 × 1.1 × 2.3	+
3	83	M	+	1.9	1.0	1.90	2.1 × 1.6 × 1.1	+
4	82	F	+	1.5	1.1	1.36	0.5 × 0.7 × 0.7	+
5	81	F	−	0.4	0.6	0.67	1.1 × 0.9 × 1.0	+
6	78	M	−	2.3	2.8	0.82	1.8 × 1.6 × 1.4	−
7	78	M	−	0.5	0.7	0.71	2.8 × 2.6 × 1.2	−
8	75	M	+	3.7	2.3	1.61	1.1 × 2.5 × 1.5	+
9	64	F	+	1.2	1.0	1.20	0.3 × 0.6 × 0.9	+
10	65	F	+	1.2	0.6	2.00	1.0 × 0.8 × 0.5	+
11	54	F	−	1.3	1.4	0.93	1.5 × 0.3 × 0.7	−
12	75	M	+	3.3	0.9	3.67	1.0 × 1.9 × 1.3	+